The Gulf of Mexico circulation inferred from surface drifters

Jonathan M. Lilly [1] Paula Pérez-Brunius [2]

[1]Theiss Research, La Jolla, California, USA [2]Departamento de Oceanografia, Centro de Investigación Científica y de Educación Superior de Ensenada (CICESE), Ensenada, Mexico

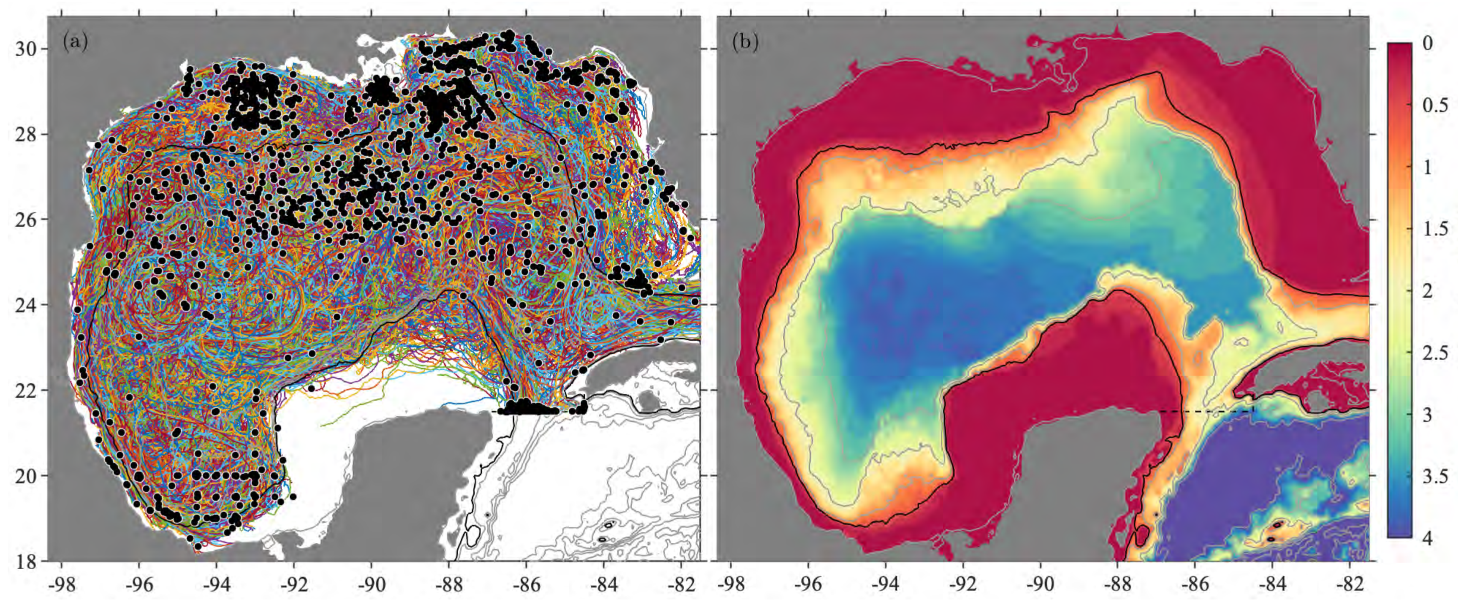

Figure 1. (a) All available surface drifter trajectories from the Gulf of Mexico, the beginning of each of which is marked by a black dot. (b) Bottom depth in the Gulf of Mexico, in kilometers. The heavy black contour is the 500 m isobath, the thin gray contour is the 5 m isobath, and the gray contours are at 1 km, 2 km, etc.

Surface Drifter Data from the Gulf of Mexico

Name	Type	Drogue	Tracking	Δ	# Traj	# Points	% Fill	First Date	Last Date	Duration	Max
(a) LATEX	WOCE	9 m	Argos	6.0	17	33792	2.201	03/08/92	19/02/95	83 ± 73	251
(b) SCULP1	CODE	1 m	Argos	1.5	378	570163	0.196	02/06/93	29/01/95	63 ± 39	131
(c) SCULP2	CODE	1 m	Argos	1.5	247	387946	0.555	06/02/96	31/10/96	65 ± 41	224
(d) GDP	SVP	15 m	Argos	6.0	73	105703	0.043	25/09/96	01/07/19	60 ± 82	403
(e) HARGOS	SVP	15 m	Argos	1.0	193	363313	2.081	20/01/99	22/04/17	78 ± 94	593
(f) AOML	CODE	1 m	Argos	Irreg.	76	76314	2.029	10/12/03	30/05/12	42 ± 25	95
(g) SGOM	FHD	45 m	GPS	1.0	459	510167	0.132	25/09/07	21/09/14	46 ± 47	254
(h) NGOM	FHD	45 m	GPS	1.0	370	461516	4.444	15/02/10	02/09/14	52 ± 48	273
(i) OCG	CODE	1 m	Argos	0.5/1.0	59	51212	0.499	30/04/10	29/01/13	36 ± 24	99
(j) GLAD	CODE	1 m	GPS	0.25	297	391442	0.004	20/07/12	22/10/12	55 ± 29	94
(k) Hercules	Tube	1 m	GPS	5 min	12	9322	3.100	27/07/13	10/09/13	32 ± 10	45
(k) HGPS	SVP	15 m	GPS	1.0	39	128090	0.169	07/08/13	31/03/19	137 ± 140	673
(m) LASER	CARTHE	1 m	GPS	0.25	996	891174	0.109	20/01/16	30/04/16	37 ± 18	89
(n) DWDE	Various	1 m	GPS	1.5	207	411172	0.574	21/06/16	18/04/18	83 ± 58	294
(o) SPLASH	CARTHE	1 m	GPS	5 min	339	101487	5.774	19/04/17	08/06/17	12 ± 11	48
(p) All	Various	Various	Various	1.0	3762	4492813	0.986	03/08/92	01/07/19	50 ± 48	673

Table 1. Meta-information for the various surface drifter datasets in the Gulf of Mexico. Δ is the nominal original sample interval in hours. The mean duration of trajectories after processing, plus or minus the standard deviation, and the maximum trajectory duration are all in days.

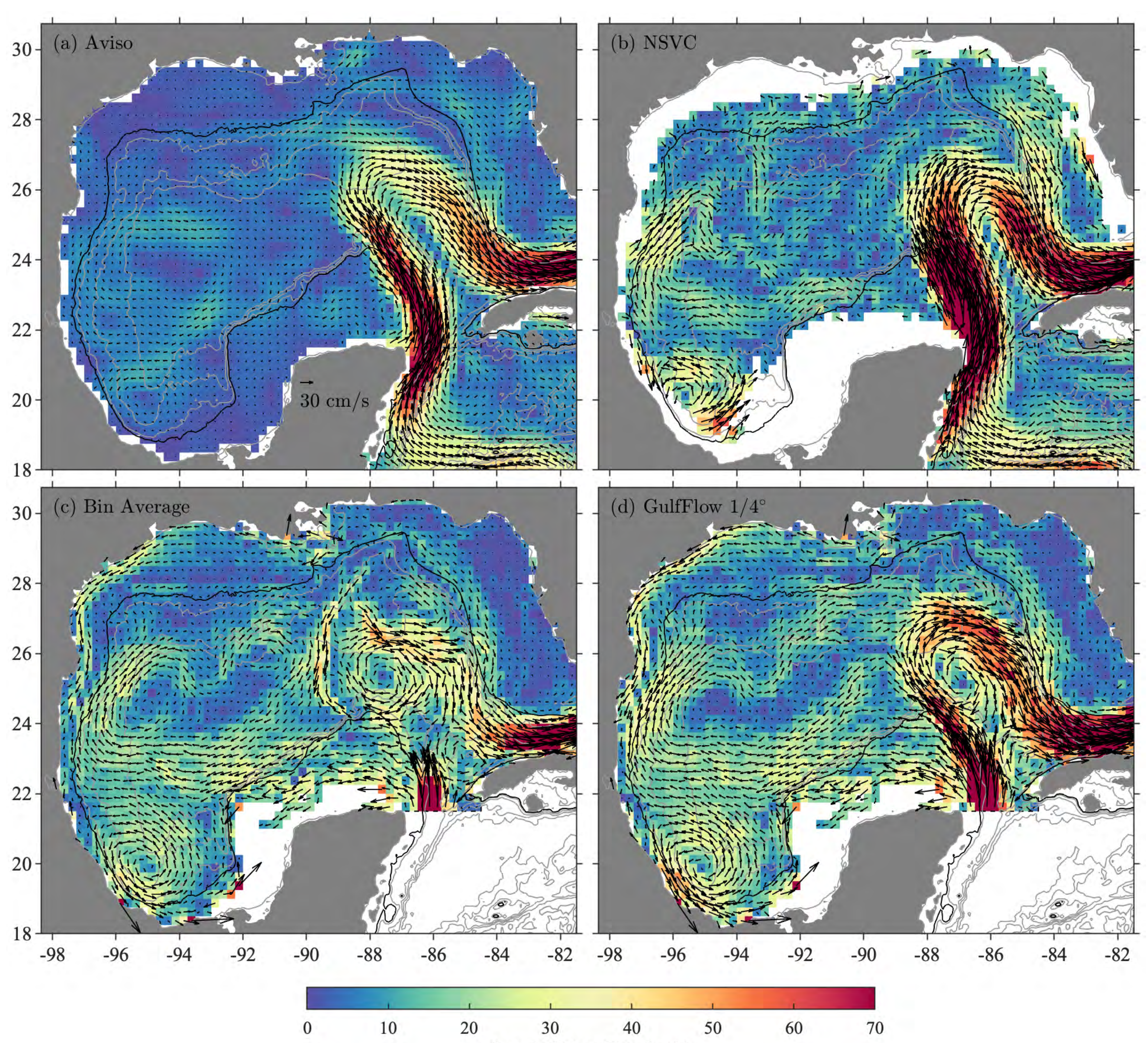

Figure 2. The mean surface circulation in the Gulf of Mexico in quarter-degree bins from (a) CMEMS (formerly Aviso) satellite altimetry, (b) the drifter-based climatology of Laurindo et al. (2017), (c) a direct bin-averaging of all drifter data from Fig. 1a, and (d) from a two-step temporal averaging of the drifter data described as in the text. Unlike the top row, no spatial smoothing is applied in the bottom row.

References

[1] L. C. Laurindo, A. J. Mariano, and R. Lumpkin.
An improved near-surface velocity climatology for the global ocean from drifter observations.
124:73–92, June 2017.

Abstract

All available surface drifter data from the Gulf of Mexico, at left in Fig. 1 and summarized in Table 1, are gathered together, uniformly processed, and used to create the highest resolution map of the mean Gulf of Mexico surface currents available to date, below in Fig. 3. In comparison to other currently available products—one from satellite altimetry in Fig. 2a and one from another drifter product in Fig. 2b—this map has far higher resolution, revealing details of the circulation that are not otherwise apparent.

Several important features are a southward-flowing coastal current on the western edge of the Gulf, a northward-flowing shelf-break current that bifurcates around 26.5°N, a strong gyre in the southern Gulf of Mexico called the Campeche Gyre, the Mississippi outflow plume, and a set of three stagnation points within the Loop Current.

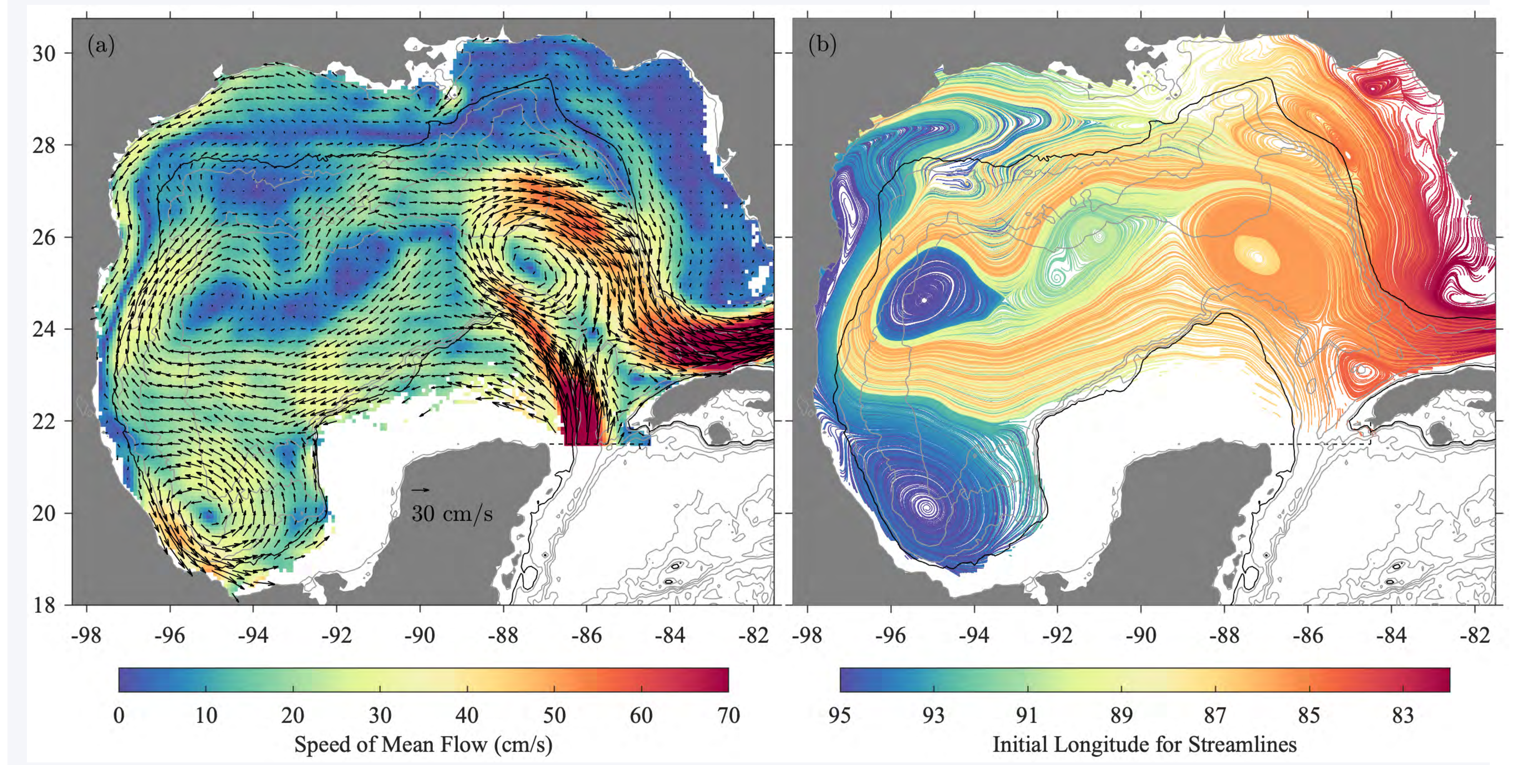

Figure 3. A high-resolution estimate of the surface circulation in the Gulf of Mexico, (a), formed as described in the text, together with (b) the corresponding streamlines colored according to their initial longitude.

To form this map one cannot simply average all available drifter data. To do so leads to Fig. 2c, which obviously has severe artifacts over the Loop Current. The explanation is found in the distribution map in Fig. 4 at right. The distortion of the Loop Current coincides with the very high sampling density from the LASER experiment.

When drifter data is distributed highly inhomogeneously in time, one does not wish to simply average it. Such an average tends to bias the result towards the state of the system at the times of densest observations.

Instead, a two-step averaging procedure is used. The drifter data from Fig. 1a is gridded spatially onto a quarter-degree grid, and temporally onto a monthly grid from August 1992 through July 2019, for 324 total "slices". Averaging this 3D gridded product over all time slices leads to the map shown in Fig. 2d, successfully removing the artifacts. Fig. 3 is formed in the same way, but with a 1/12° degree spatial grid and a final smoothing within 50 km radius circles using a parabolic weighting function.

The improvement from this averaging approach can be quantified. Sampling CMEMS altimetry, as well as the output of three different 20-year high-resolution model simulations of the region, at the space/time locations of the observed trajectories, we then estimate the mean currents using (I) a straight bin-averaging or (II) the two-step time-slice averaging. Errors can be quantified because the true mean fields are known.

The mean fields for these four products are shown in Fig. 5, while the reconstructed mean fields are shown in Fig. 6. The errors, presented in Table 2, indicate a 32% to 44% percent reduction in error due to this simple change in the averaging method.

Mean Flow Estimation Error Assessment

Velocity	RMS error I	RMS error II	Reduction
AVISO	13.6 cm s^{-1}	8.6 cm s^{-1}	36.9%
HYCOM	12.1 cm s^{-1}	8.2 cm s^{-1}	32.1%
NEMO	10.9 cm s^{-1}	7.2 cm s^{-1}	33.6%
ROMS	18.5 cm s^{-1}	10.4 cm s^{-1}	44.0%

Table 2. Errors in estimating the mean flow using two different time-averaging schemes, (I) straight bin averaging and (II) two-step time-slice averaging, as well as the error reduction associated with the latter.

In addition to yielding a much improved estimate of the Gulf surface currents, these results point to a basic yet perhaps unappreciated problem that arises when working with Lagrangian data. This approach could be explained on theoretical grounds, and optimized, by considering Eulerian decorrelation times.

Future work involves investigating the seasonal and interannual variability contained within the 3D gridded drifter dataset.

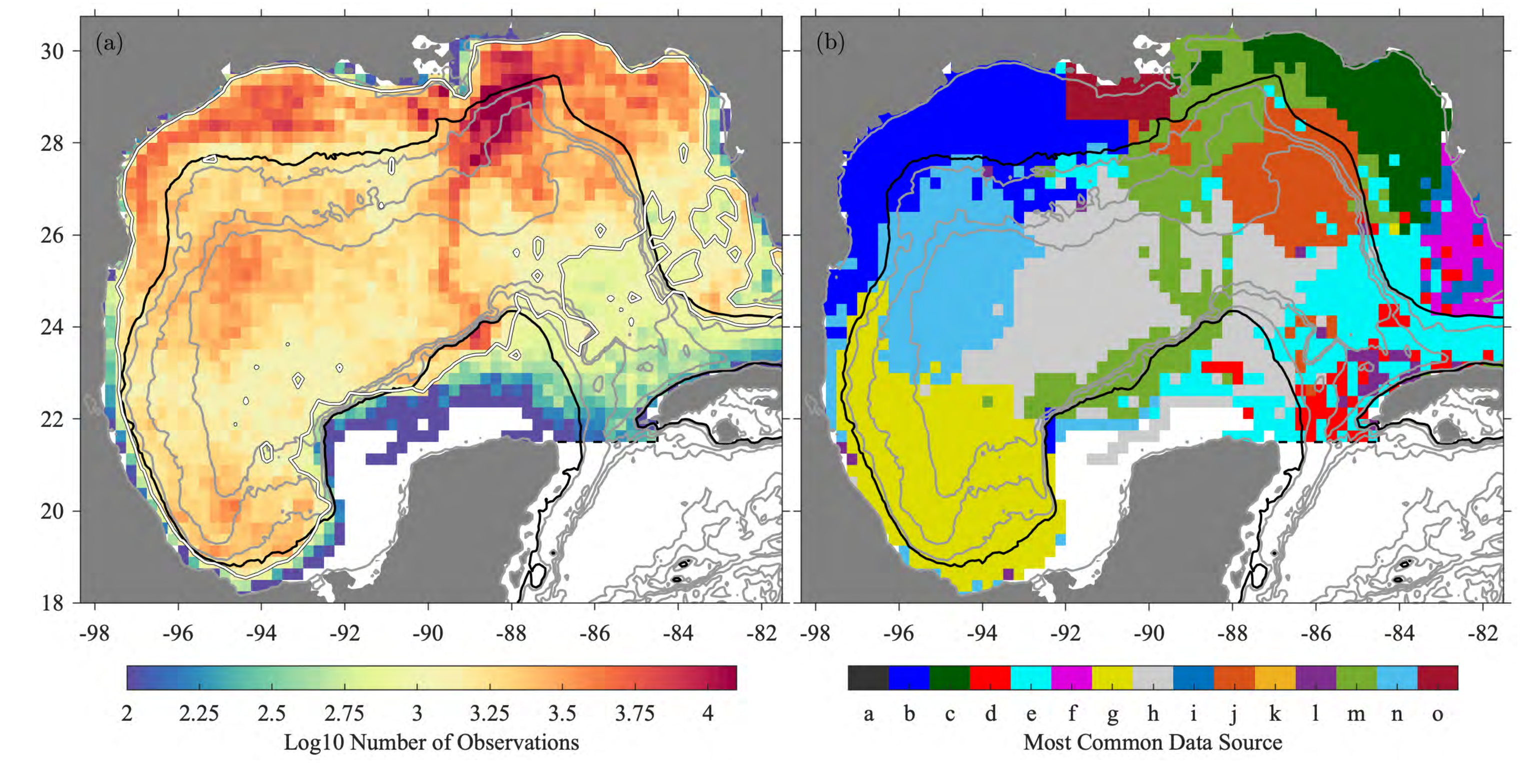

Figure 4. The number of hourly drifter observations from Fig. 1a in quarter-degree bins presented on a logarithmic scale, in (a), together with (b) the most common data source within each bin.

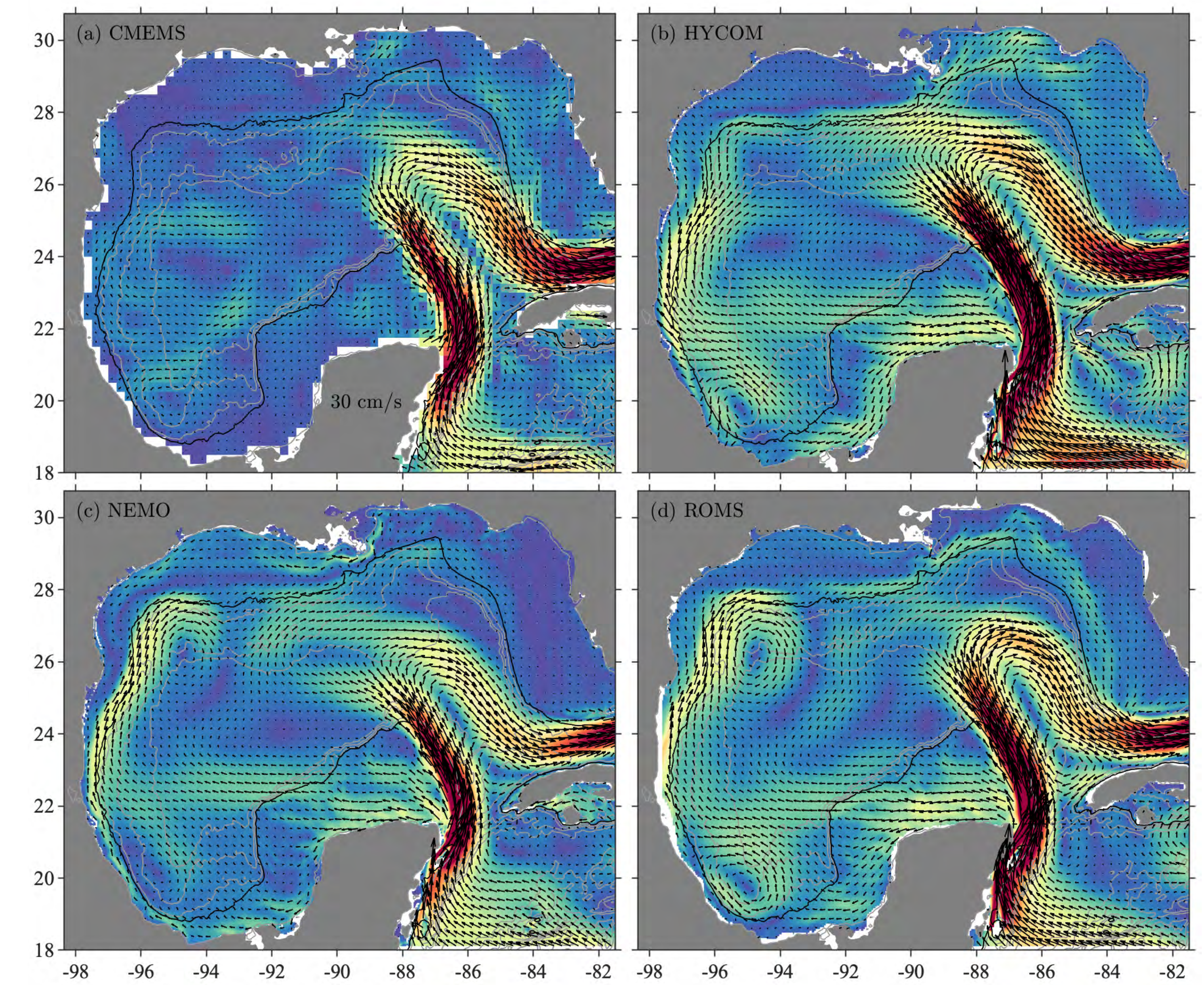

Figure 5. Time-mean surface currents for (a) CMEMS, (b) HYCOM, (c) NEMO, and (d) ROMS.

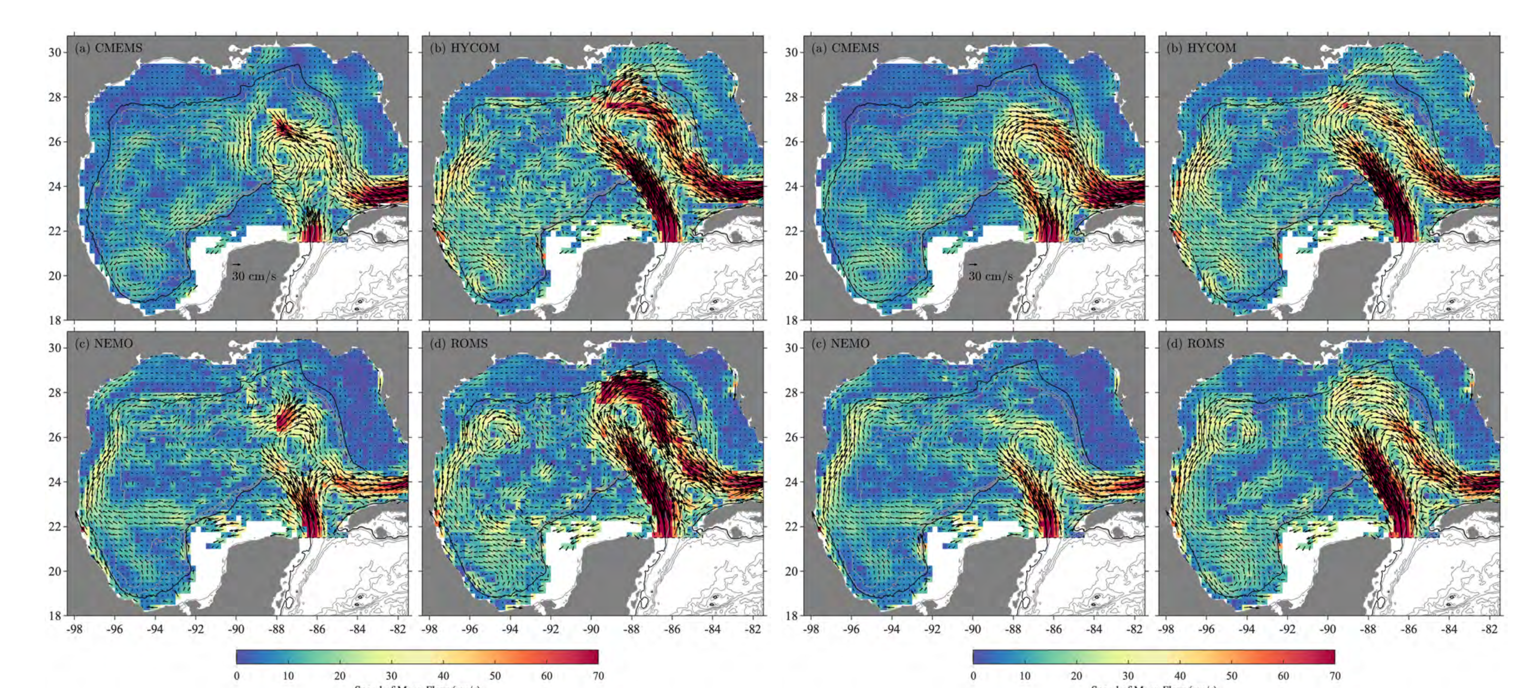

Figure 6. Reconstructions of the velocity fields in Fig. 5 from velocity data extracted along the observed drifter trajectories using (I) straight bin averaging, at left, or (II) two-step time-slice averaging, at right.

Acknowledgments

20-year model runs kindly provided by CIGoM Numerical Modeling Group (CICESE, CCA-UNAM, LEGOS). This research has been funded by the Mexican National Council for Science and Technology - Mexican Ministry of Energy - Hydrocarbon Fund, project 201441. This is a contribution of the Gulf of Mexico Research Consortium (CIGoM). We acknowledge the specific request by Petróleos Mexicano (Pemex) to the Hydrocarbon Fund to address the environmental effects of oil spills in the Gulf of Mexico that made this project possible.